Supplemental information for Geometric confinement guides topological defect pairings and emergent flow in nematic cell populations

Ryo Ienaga,[1] Kazusa Beppu,[2] and Yusuke T. Maeda[1,*]

[1]*Department of Physics, Kyushu University, Motooka 744, Fukuoka 819-0395, Japan*
[2]*Department of Applied Physics, Aalto University School of Science, Puumiehenkuja 2, Espoo, 02150, Finland*

(Dated: June 20, 2023)

Supplementary information text

Supplementary movies

- Movie S1. Time-lapse movie of collective motion of C2C12 cells in a flat two-dimensional surface. Scale bar, 100 µm.

- Movie S2. Time-lapse movie of growing orientational correlation and defects annihilation. Scale bar, 100 µm.

- Movie S3. Time-lapse movie of collective motion and orientation field of C2C12 cells confined in a doublet circle boundary ($\Delta/R = 1.83$). Scale bar, 100 µm.

- Movie S4. Time-lapse movie of collective motion and orientation field of C2C12 cells confined in a triplet circle boundary ($\Delta/R = 1.83$). Scale bar, 100 µm.

Cell movement along the circular boundary

We conducted an analysis of the cell motion in the vicinity of a curved boundary within a circular confinement. The cell population was confined within circular boundaries of various size $R = 200, 250, 300$, and 350 µm. The motion of single cells was tracked using particle tracking velocimetry analysis, and the tangential velocity ($\boldsymbol{v}_{PTV} \cdot \boldsymbol{t}$) along the tangential direction ($\boldsymbol{t}$) of the circular boundary was analyzed for cells located near the boundary. The resulting tangential velocity was then plotted for each radius R (Figure S2). If the scaled tangential velocity ($\frac{|\boldsymbol{v}_{PTV} \cdot \boldsymbol{t}|}{||\boldsymbol{v}_{PTV}||}$) is 1, the cells move parallel to the boundary. Conversely, if the normalized tangential velocity is 0, the cells move in the normal direction. We found that the scaled tangential velocity remained consistently at 0.8 for any confinement size R, indicating that the cells were oriented parallel to the tangent line in the vicinity of the boundary.

The effect of myosin-inhibition

The C2C12 cells enclosed within the boundary geometry exhibit a negative velocity divergence ($\nabla \cdot \boldsymbol{v}$), as depicted in Figure 4 of the main text. The motility of these cells is suppressed by the inhibition of myosin molecular motors, which generate contractile force, resulting in a decay of velocity. To investigate the impact of the myosin molecular motor on the negative velocity divergence, we suppressed motor activity using blebbistatin (10 μM) and analyzed the collective motion under boundary confinement. While the value of velocity divergence remained negative, its magnitude was diminished in comparison to the case without myosin inhibition.

*Electronic address: ymaeda@phys.kyushu-u.ac.jp

The effect of cell division inhibition

Cell population with inhibited cell division was prepared by treating the cells with mitomycin C (10 μg/mL) for 1 hour. The collective motion of division-inhibited cells was then recorded for 48 hours to analyze the velocity field, orientation field (and topological defects), as well as to measure the cell number density (Figure S5(a)-(c)). The results showed that negative velocity divergence was observed with paired +1/2defects facing each other. (Figure S5(a)-(b)). Although cell division was inhibited, the number density was higher near the center, yet less than half of that in the control condition (Figure S5(c)-(d)). This finding indicates a negative correlation between cell number density and velocity divergence (Figure S5(e)), which confirms that the inhibition of cell division does not affect the pattern of topological defects or inward flow of confined cells.

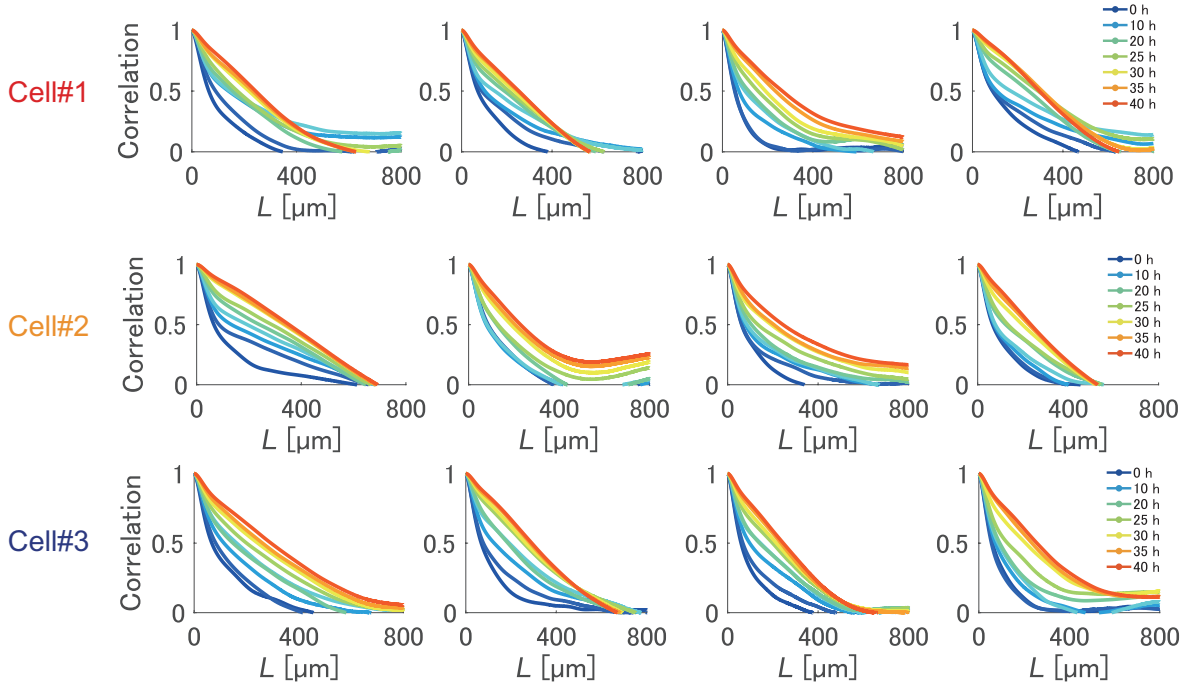

FIG. S1: **Autocorrelation function of the orientation field in unconstrained C2C12 populations**. We show the autocorrelation function of the orientation field, $C(L,t)$, utilized for Figures 1(m) and 1(n) of the main text. Four different locations were measured at a distance of at least 1 mm for each measurement, and the correlation function at each site are exhibited.

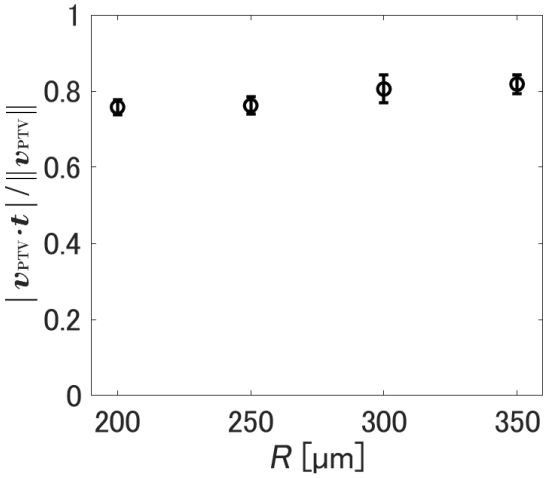

FIG. S2: **Single cell motion along the edge of circular pattern**. The normalized tangential velocity is plotted with the radius of a circular confinement R.

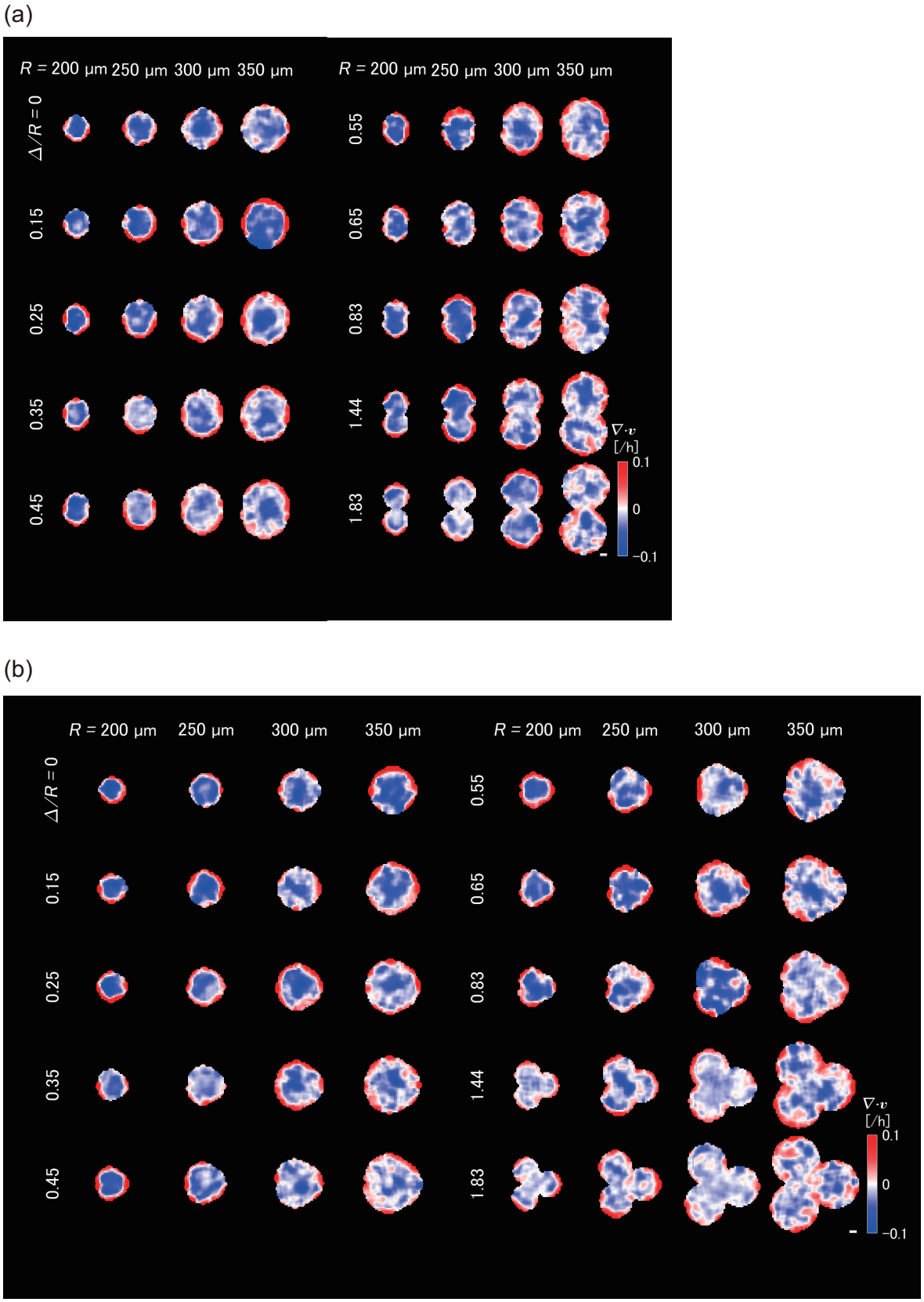

FIG. S3: **(a and b)** Divergence of velocity field in confined cell populations. Scale bars: 100 μm. Typical examples of velocity divergence $\nabla \cdot \boldsymbol{v}$ are shown for each geometric condition in (a) doublet circle pattern and (b) triplet circle pattern. The geometric constraint is a circle having radius R =200, 250, 300 and 350 μm and ten patterns with Δ/R =0, 0.15, 0.25, 0.35, 0.45, 0.55, 0.65, 0.83, 1.44, and 1.83.

(c)

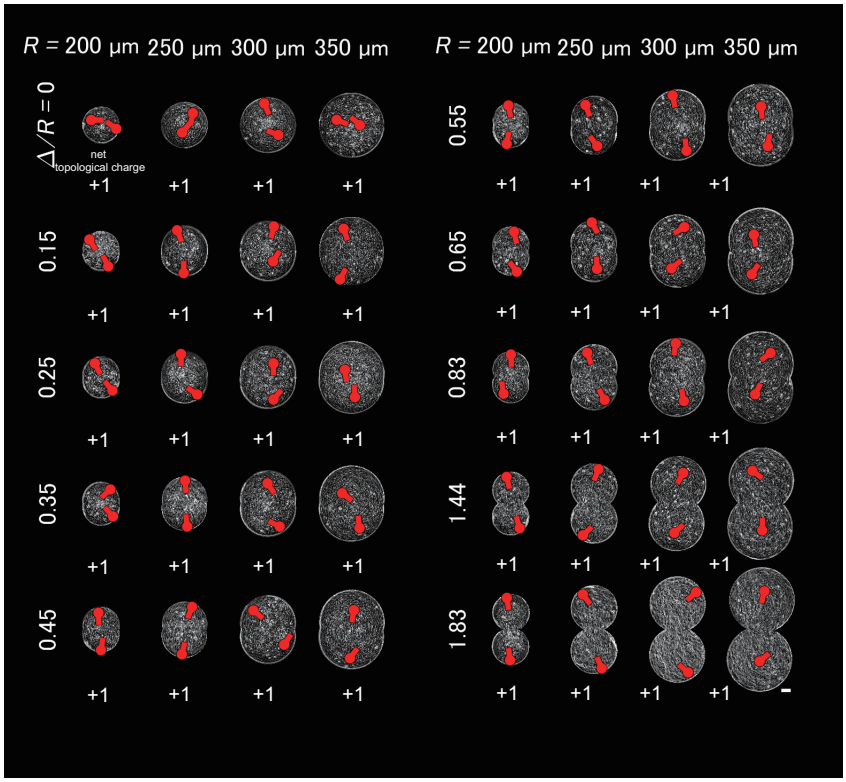

(d)

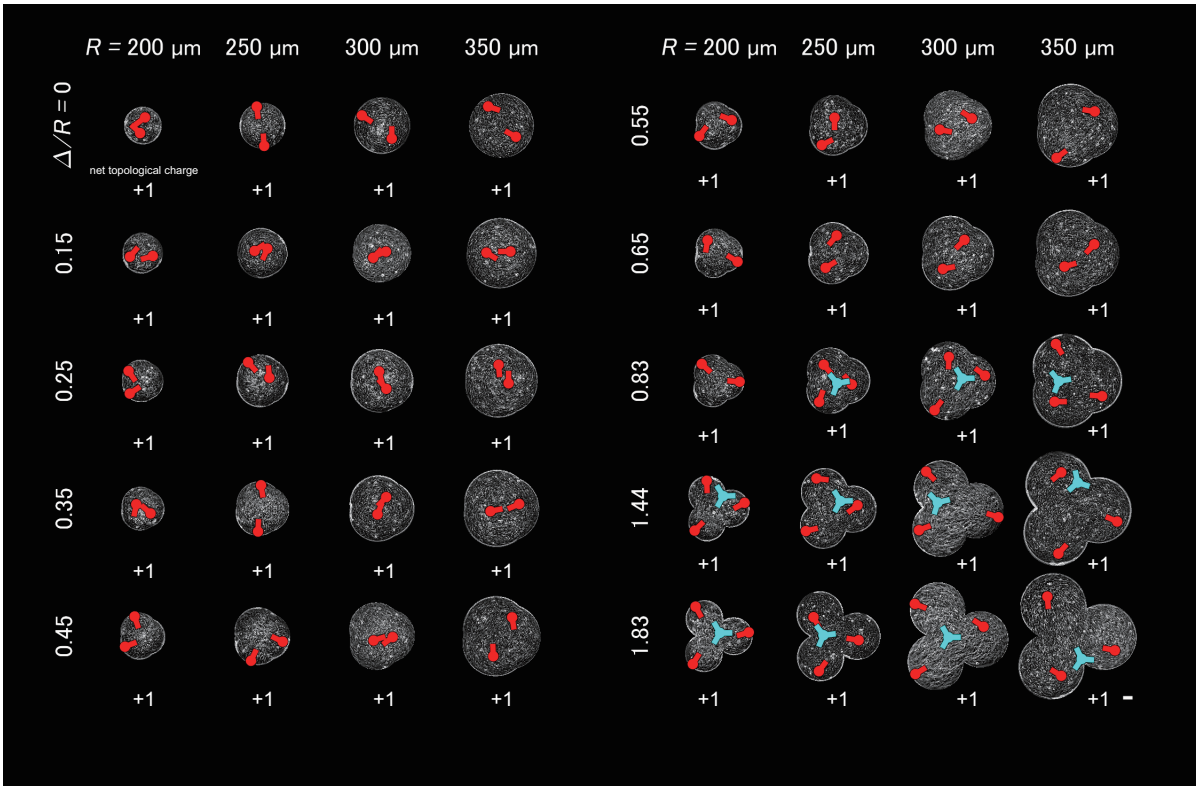

FIG. S3: **(c and d)** Phase contrast images of confined cell populations. Scale bars: 100 μm. Typical examples of confined cells with topological defects are shown for each geometric condition in (c) doublet circle pattern and (d) triplet circle pattern. The geometric constraint is a circle having radius R =200, 250, 300 and 350 μm and ten patterns with Δ/R =0, 0.15, 0.25, 0.35, 0.45, 0.55, 0.65, 0.83, 1.44, and 1.83.

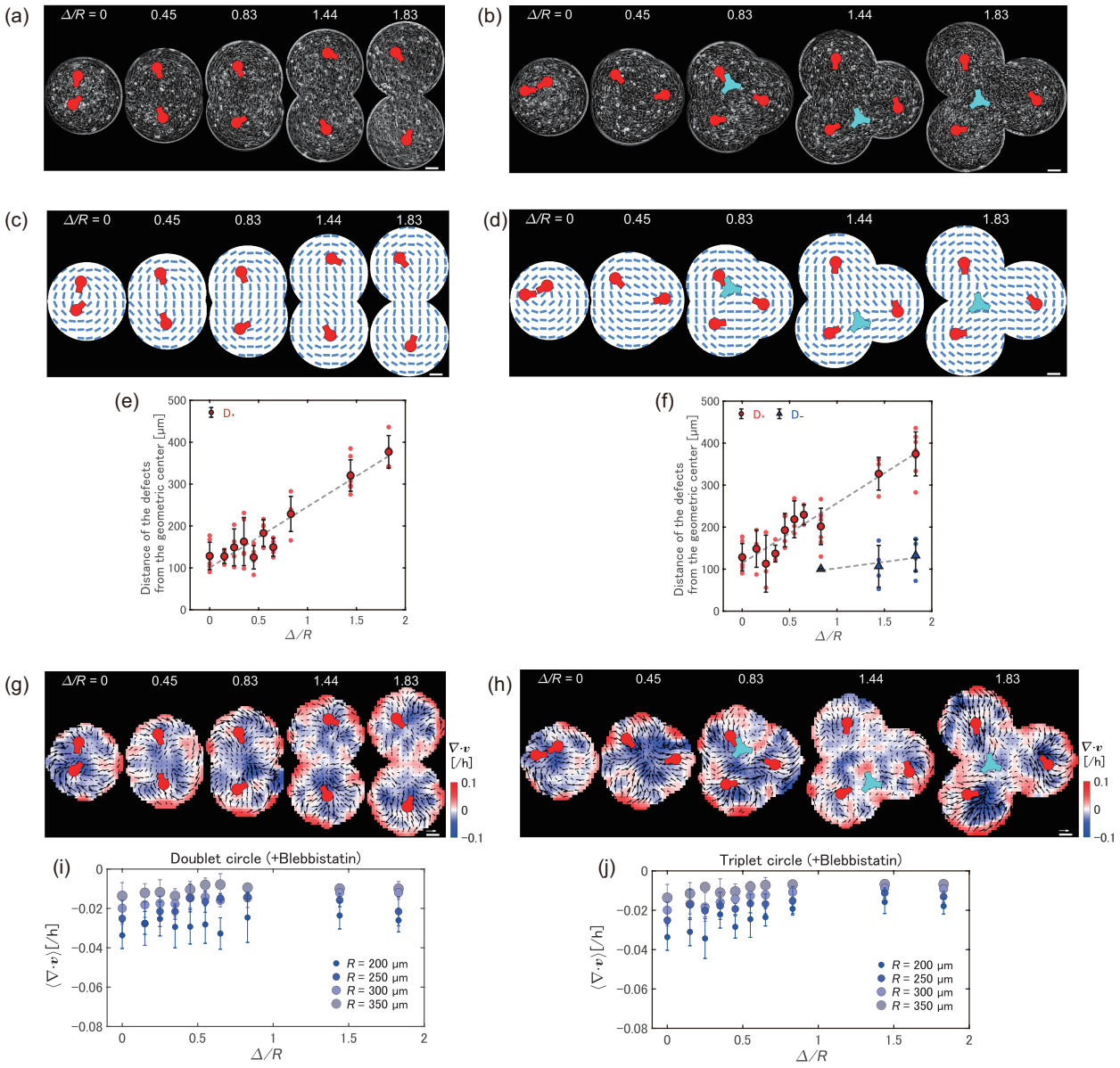

FIG. S4: **The effect of myosin inhibition on topological defects pairing and negative velocity divergence.** (a, c, e, g, h) doublet circle pattern, and (b, d, f, h, j) triplet circle pattern. Scale bars: 100 μm. **(a and b)** Phase contrast image of confined C2C12 cells treated with 10 μM blebbistatin (myosin inhibitor). **(c and d)** Corresponding director field analyzed from (a) and (b). **(e and f)** The distance of half-integer defects from the center of doublet circle pattern with $R = 300\,\mu$m. $+1/2$ defects (D_+, red circle) and $-1/2$ defects (D_-, blue triangle). Error bars represent the standard deviation. **(g and h)** Velocity divergence $\boldsymbol{\nabla} \cdot \boldsymbol{v}$ in confined myosin-inhibited cells. **(i and j)** The mean value of velocity divergence $\boldsymbol{\nabla} \cdot \boldsymbol{v}$ within the confined space. Error bars represent the standard deviation.

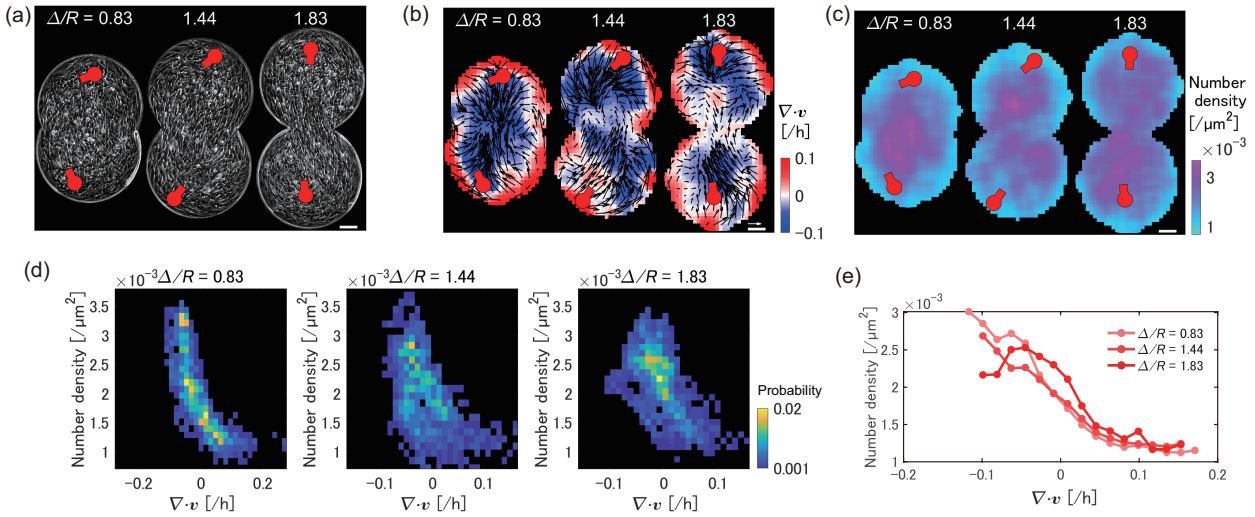

FIG. S5: **The effect of cell division inhibition on negative velocity divergence and topological defects pairing in confined C2C12 cells.** The cell populations confined in doublet circle patterns are shown as representative data. Scale bars: 100 μm. **(a)** phase contrast images, **(b)** Velocity divergence, and **(c)**Cell number density in confined C2C12 cells treated with mitomycin C. $\boldsymbol{\nabla} \cdot \boldsymbol{v}$ in confined C2C12 cells under cell division inhibition. **(d)** Probability distribution map of cells for velocity divergence and cell number density at geometric conditions $\Delta/R = 0.83, 1.44$, and 1.83. **(e)** The average cell density as a function of velocity divergence was analyzed. The horizontal axis representing velocity divergence was fractionated into intervals of 0.01 [1/h], and the average cell number density within each interval was plotted.

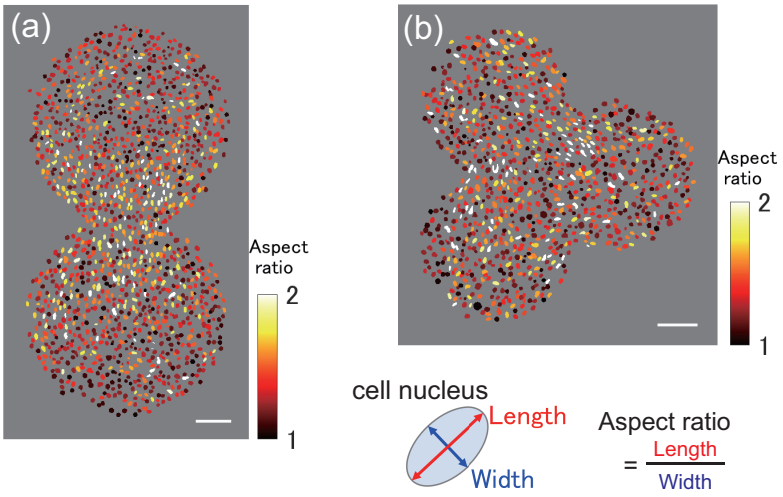

FIG. S6: **The deformation of cell nucleus in confined C2C12 cells.** The spatial map of the cell nucleus under the confinement of (a) doublet circle pattern and (b) triplet circle pattern at $\Delta/R = 1.83$. The representative fluorescent images taken at 48 hours are shown with color code for aspect ratio. The aspect ratio is defined as the ratio of major length (length) to minor length (width) of the cell nucleus. The large aspect ratio in white color indicates stretched nucleus shape. Scale bars: 100 μm.